In vivo diagnosis of murine pancreatic intraepithelial neoplasia and early-stage pancreatic cancer by molecular imaging

Stefan Eser[a,1], Marlena Messer[a,1], Philipp Eser[b], Alexander von Werder[a], Barbara Seidler[a], Monther Bajbouj[a], Roger Vogelmann[a], Alexander Meining[a], Johannes von Burstin[a], Hana Algül[a], Philipp Pagel[b], Angelika E. Schnieke[c], Irene Esposito[d], Roland M. Schmid[a], Günter Schneider[a], and Dieter Saur[a,2]

[a]II. Medizinische Klinik, Technische Universität München, 81675 Munich, Germany; [b]Lehrstuhl für Genomorientierte Bioinformatik and [c]Livestock Biotechnology, Technische Universität München, Wissenschaftszentrum Weihenstephan, 85354 Freising, Germany; and [d]Institute of Pathology, Technische Universität München, 81675 Munich, Germany

Edited by David A. Cheresh, University of California at San Diego, La Jolla, CA, and accepted by the Editorial Board May 6, 2011 (received for review January 18, 2011)

Pancreatic ductal adenocarcinoma (PDAC) is a fatal disease with poor patient outcome often resulting from late diagnosis in advanced stages. To date methods to diagnose early-stage PDAC are limited and in vivo detection of pancreatic intraepithelial neoplasia (PanIN), a preinvasive precursor of PDAC, is impossible. Using a cathepsin-activatable near-infrared probe in combination with flexible confocal fluorescence lasermicroscopy (CFL) in a genetically defined mouse model of PDAC we were able to detect and grade murine PanIN lesions in real time in vivo. Our diagnostic approach is highly sensitive and specific and proved superior to clinically established fluorescein-enhanced imaging. Translation of this endoscopic technique into the clinic should tremendously improve detection of pancreatic neoplasia, thus reforming management of patients at risk for PDAC.

molecular in vivo imaging | early detection | carcinoma in situ | genetically engineered mouse model | cathepsin

Pancreatic cancer (pancreatic ductal adenocarcinoma, PDAC) is one of the deadliest human malignancies, with an extremely poor 5-y survival rate below 5% (1). Because patients generally present with symptoms relating to late stages of the disease, diagnosis of resectable PDAC is achieved in less than 15% of cases (1). However, investigators have reported that diagnosis and resection of early-stage PDAC (<2 cm in size) can result in a 4-y survival rate of up to 78% (2–5). These data suggest that early detection of PDAC can improve patient outcome. In addition, it has been shown that resection of PDAC combined with adjuvant chemotherapy can improve 5-y survival rates to 25%. Thus, increasing the chance of resection will lead to improved survival.

Of the more than 33,000 new cases of PDAC diagnosed in the United States every year, ~10% occur in families with a high prevalence of PDAC and are thus referred to as familial (6, 7). In a cohort study of twins, it was proposed that inherited factors may be responsible for up to 36% of pancreatic cancers, suggesting that the incidence of familial pancreatic cancer may be even higher than presently assumed (8). To date, several conditions associated with familial PDAC have been described and groups of individuals at low, moderate, or high risk for developing the disease have been defined (9, 10). Although clinical trials are currently testing screening protocols for the high-risk group, aimed at detecting curable precursors of PDAC such as intraductal papillary mucinous neoplasia, pancreatic intraepithelial neoplasia (PanIN), and early-stage PDAC (10–12), the results of these trials show that early lesions are often missed. Furthermore, false positive findings can lead to overtreatment of a significant fraction of the screened population (12). These findings show that better diagnostic tools for the detection of preneoplastic lesions and early-stage PDAC are urgently needed. Recent data demonstrate that preinvasive precursors progress slowly over many years to decades to invasive pancreatic cancer (13). The parental pancreatic cancer founder clone then requires more than 5 y to acquire the capacity to metastasize (13). Thus, there is a time frame of several years for the diagnosis of curable disease, implicating the need for sensitive diagnostics.

In the current study, we investigated a relevant genetically engineered $Kras^{G12D}$-dependent endogenous mouse model of murine PanIN (mPanIN) development and progression to PDAC, which accurately recapitulates the human disease (14, 15). By using a cathepsin-activatable near-infrared (NIRF) probe in combination with confocal fluorescence lasermicroscopy (CFL) we were able to detect early-stage PDAC as well as mPanIN lesions in vivo on the cellular level. Furthermore, it was possible to differentiate between normal pancreatic tissue and low-grade mPanINs on the one hand and high grade mPanINs and early-stage PDAC on the other, illustrating the great potential of this technique in the diagnosis of curable precursors and early-stage PDAC.

Results

Identification of Cathepsins as Targets for Molecular Imaging of PanIN Lesions and Early-Stage PDAC. To identify targets for molecular imaging of PanIN lesions and early-stage PDAC we used genomewide pancreatic gene expression analyses of $Ptf1a^{Cre/+}$; $LSL\text{-}Kras^{G12D/+}$ mice, littermate controls, as well as mice with acute caerulein-induced pancreatitis. Expression profiles of over 30 individual mice revealed high levels of cathepsins B, H, L, and S in all mice with mPanIN lesions or early-stage PDAC (Fig. 1*A*). In contrast, expression of these cathepsins was low in normal and inflamed pancreatic tissue (Fig. 1*A*). To validate expression of cathepsins and to examine the localization of the corresponding proteins, we performed immunohistochemistry. Strong staining for cathepsins B, H, L, and S was detected in preinvasive mPanIN lesions and PDAC (Fig. 1*B*). In line with the microarray mRNA expression data, minimal cathepsin B, H, L, and S staining was observed in normal and inflamed pancreatic tissue (Fig. 1*B*). Furthermore, immunohistochemical staining of human pancreatic tissue sections also revealed high expression of cathepsins B, H, L, and S in PanIN lesions and PDAC (Fig. S1 and Table S1).

Author contributions: D.S. designed research; S.E., M.M., A.v.W., B.S., M.B., and D.S. performed research; P.E., H.A., P.P., I.E., and R.M.S. contributed new reagents/analytic tools; S.E., M.M., P.E., A.v.W., B.S., M.B., R.V., A.M., J.v.B., P.P., A.E.S., I.E., G.S., and D.S. analyzed data; and S.E., G.S., and D.S. wrote the paper.

The authors declare no conflict of interest.

This article is a PNAS Direct Submission. D.A.C. is a guest editor invited by the Editorial Board.

[1]S.E. and M.M. contributed equally to this work.

[2]To whom correspondence should be addressed. E-mail: Dieter.Saur@lrz.tum.de.

This article contains supporting information online at www.pnas.org/lookup/suppl/doi:10.1073/pnas.1100890108/-/DCSupplemental.

MEDICAL SCIENCES

Downloaded at Palestinian Territory, occupied on November 26, 2021

www.manaraa.com

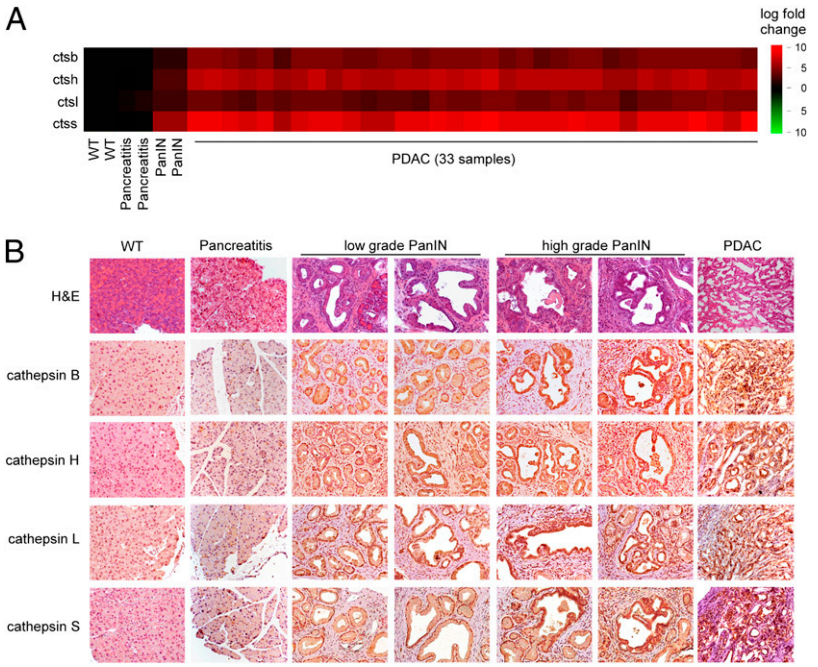

Fig. 1. Cathepsins are highly expressed in preinvasive mPanIN lesions and early-stage PDAC. (*A*) mRNA expression profiling of pancreatic tissues from wild-type controls (WT), mice with caerulein-induced pancreatitis, and *Ptf1a*$^{Cre/+}$;*LSL-Kras*$^{G12D/+}$ mice bearing mPanINs and PDAC, respectively. RNA was isolated from tissue specimens, labeled, and hybridized onto a GeneChip Mouse Genome 430 2.0 array (Affymetrix). Expression levels of cathepsin proteases are shown as log-fold change in row-*Z* scale (ctsb, cathepsin B; ctsh, cathepsin H; ctsl, cathepsin L; ctss, cathepsin S). (*B*) Paraffin-embedded pancreatic tissue sections from wild-type mice, caerulein-treated mice with pancreatitis, and *Ptf1a*$^{Cre/+}$;*LSL-Kras*$^{G12D/+}$ mice with mPanIN lesions and PDAC were stained for ctsb, ctsh, ctsl, and ctss.

Together, these data suggest that cathepsins B, H, L, and S are highly expressed in human and murine PanINs and PDAC and thus represent suitable targets for a molecular imaging-based diagnostic approach.

Activation of the Cathepsin-Activatable NIRF Probe in mPanIN Lesions and Early-Stage PDAC. Cathepsins B, H, L, and S are activators of an established NIRF probe that is based on fluorescence resonance energy transfer (16–18). To test this cathepsin-activatable NIRF probe in vivo, we injected it into *Ptf1a*$^{Cre/+}$;*LSL-Kras*$^{G12D/+}$ mice bearing mPanIN lesions or early-stage PDAC. Twenty-four hours after i.v. injection, cryosamples of the respective pancreata were prepared and sections were imaged on an Odyssey planar near-infrared scanner to detect the signal of the NIRF probe (Fig. 2*A*). Tissue sections showed a strong signal emitted by the cleaved NIRF probe in mPanINs and PDAC, proving specific activation of the probe (Fig. 2*A*). In contrast, normal pancreatic tissues from wild-type mice and pancreatic tissues from mice with acute pancreatitis showed only weak and focal activation of the NIRF probe (Fig. 2 *A* and *C*). Hematoxylin and eosin (H&E) staining of the scanned cryosections revealed that the signal of the NIRF probe was emitted from neoplastic tissue (Fig. 2*B*). No NIRF-probe signal was detected in areas of tumor necrosis, demonstrating the specificity of the NIRF probe for vital tumor tissue (Fig. 2*B*).

To investigate activation of the cathepsin-activatable NIRF probe on a cellular level ex vivo, we performed confocal laser-scanning microscopy. Cryosections were stained for morphology using an anti–E-cadherin antibody and simultaneously imaged for the NIRF-probe signal. This signal was specifically present in neoplastic cells of mPanIN lesions and early-stage PDAC (Fig. 2*D*). Notably, signal intensity increased from low to high grade mPanIN lesions and was strongest in PDAC. In line with our previous findings only marginal activation of the NIRF probe was found in the controls (16) (Fig. 2*D*). Mice with pancreatitis showed presence of the signal in immune cells that could be clearly distinguished from neoplastic cells due to differences in cell morphology and staining pattern (Fig. 2*D*).

Early Diagnosis of Pancreatic Cancer and mPanIN Lesions by CFL in Vivo. To evaluate the NIRF probe for detection of mPanINs and PDAC in vivo, we used the genetically defined Kras^{G12D}-dependent endogenous mouse model. In vivo CFL was performed after i.v. administration of the NIRF probe to 1, 3, 6, 9, and 12 mo old *Ptf1a*$^{Cre/+}$;*LSL-Kras*$^{G12D/+}$ mice displaying the whole range of mPanIN grades and early-stage PDAC and wild-type littermate controls with no morphological changes (Fig. 3*A*). For CFL imaging the fiber optic miniprobe was placed in contact with the pancreas, which allows single-cell resolution imaging and thus grading of mPanIN lesions. The intensity of the NIRF-probe signal detected by CFL increased with mPanIN progression to PDAC and correlated well with histological alterations in corresponding matched H&E stained sections of imaged pancreata. Importantly, CFL allowed morphological characterization of the individual cells comprising the lesion and a clear differentiation between neoplastic cells and immune cells (Fig. 3*A* and Movies S1, S2, S3, S4, S5, S6, S7, and S8). Ex vivo whole organ scans using the Odyssey near-infrared reader verified these findings on a macroscopic level, further illustrating the correlation of the NIRF-probe signal intensity with disease progression (Fig. 3*B*).

Molecular Imaging of mPanIN Lesions and Early-Stage PDAC in Vivo by Combined Dual Wavelength Imaging of Cathepsin Activity and Vascularity. Because the nonspecific vascular contrast agent fluorescein is approved for clinical use in humans including endoscopic flexible lasermicroscopic imaging of neoplasia in the gastrointestinal tract (19), we wished to compare and combine the diagnostic power of the specific cathepsin-activatable NIRF probe with that of fluorescein. By using fluorescein for in vivo CFL imaging, normal pancreatic tissue architecture could be visualized well on a cellular level (Fig. 4*A* and Movie S1). However, no clear

Downloaded at Palestinian Territory, occupied on November 26, 2021
www.manaraa.com

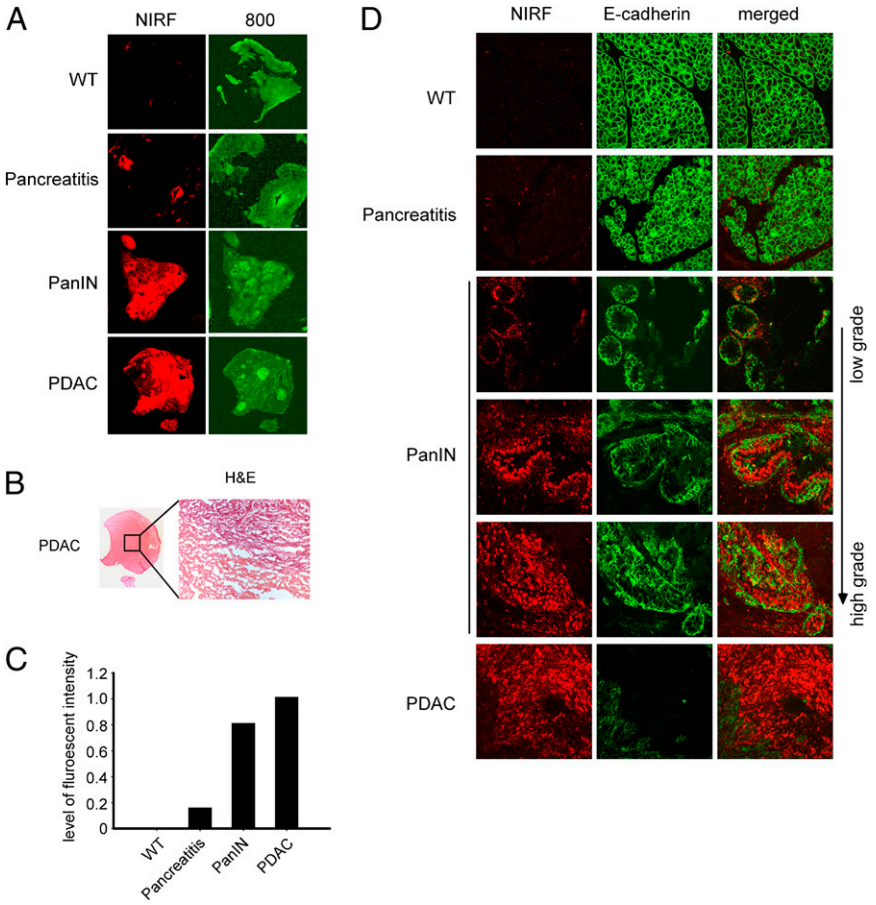

Fig. 2. Specific activation of a cathepsin-sensitive NIRF probe in mPanIN lesions and PDAC. (*A*) Near-infrared (NIRF) imaging of pancreatic tissues from *Ptf1a*$^{Cre/+}$;*LSL-Kras*$^{G12D/+}$ mice bearing mPanIN lesions and PDAC. Wild-type (WT) littermates and mice with caerulein-induced acute pancreatitis served as controls. Tissues were harvested 24 h after i.v. injection of the cathepsin-activatable NIRF probe. Cryosections were then scanned with a planar Odyssey near-infrared reader at 680 nm for visualization of the NIRF probe. The NIRF-probe signal is shown in red. Bright field imaging (green color) to show morphology was performed at 800 nm. (*B*) Histological analysis of the serial section of the scanned PDAC specimen depicted in *A* shows necrosis next to viable tumor, correlating with the NIRF-probe signal (magnification: left, 2×; right, 200×). (*C*) Quantification of fluorescence intensity in scanned cryosections shown in *A* using Odyssey software. (*D*) Confocal lasermicroscopic imaging of activated cathepsin-sensitive NIRF probes in cryosections from normal pancreas, caerulein-induced pancreatitis, low- and high-grade mPanIN lesions, and PDAC (magnification, 200×). The signal from the activated NIRF probe is depicted in red. E-cadherin counterstain displays morphology (green).

discrimination between low- and high-grade mPanIN lesions and early-stage PDAC was possible. This lack of discrimination was mainly due to fibrosis, which is associated with all grades of mPanIN lesions as well as early-stage PDAC (Fig. 4*A* and Movies S1, S2, S3, and S4). In contrast, the specific cathepsin-activatable NIRF probe allows clear differentiation between normal pancreas, low-grade mPanIN lesion, high-grade mPanIN lesion, and early-stage PDAC on the cellular level (Figs. 3*A* and 4*B* and Movies S5, S6, S7, and S8). High-grade mPanIN lesions were specifically characterized and distinguished from low-grade mPanINs and normal or inflamed pancreatic tissue by increased signal intensity of the NIRF probe and a typical ductal-like pattern of activation produced by cells of differing shape and size (Figs. 3*A* and 4*B* and Movies S5, S6, S7, and S8). In early-stage PDAC, the strong intensity of the NIRF-probe signal together with disturbed tissue architecture and a heterogeneous activation pattern generated by aberrant neoplastic cells allowed the differentiation from normal pancreatic tissue, infiltrating immune cells and all grades of mPanIN (Figs. 3*A* and 4*B* and Movies S5, S6, S7, and S8). The single-cell resolution of CFL imaging enabled an in vivo histopathological diagnosis based on the cellular morphology of mPanINs and PDAC. The combination with the vascular contrast agent fluorescein provided additional morphological information about the pancreas, especially about fibrosis, but did not improve accuracy of diagnosing mPanINs and PDAC in vivo. These findings demonstrate that the use of CFL in combination with the highly specific cathepsin-activatable NIRF probe is superior to fluorescent imaging of blood vessels alone and allows the accurate diagnosis of neoplastic precursor lesions and early-stage PDAC by in vivo histopathology.

Detection and Grading of mPanIN Lesions and Early-Stage PDAC by in Vivo Imaging of Cathepsin Activity in a Double Blind Study. To investigate the sensitivity and specificity of CFL imaging of cathepsin activity to detect and grade mPanIN lesions and PDAC, we conducted a double blinded in vivo study. CFL was performed in a total of 24 mice with the investigators being unaware of the genotype and age of each individual animal and at least six representative films were recorded. The study group included 6 age-matched wild-type control mice and 18 *Ptf1a*$^{Cre/+}$;*LSL-Kras*$^{G12D/+}$ mice with ages varying from 43 to 389 d. On the basis of the laser microscopic sequences, two independent examiners blinded to the histological results, graded mPanIN lesions and PDAC. Finally, a histopathological diagnosis was made by a third independent blinded investigator. The third investigator evaluated and scored the corresponding serial histological sections unaware

Downloaded at Palestinian Territory, occupied on November 26, 2021
www.manaraa.com

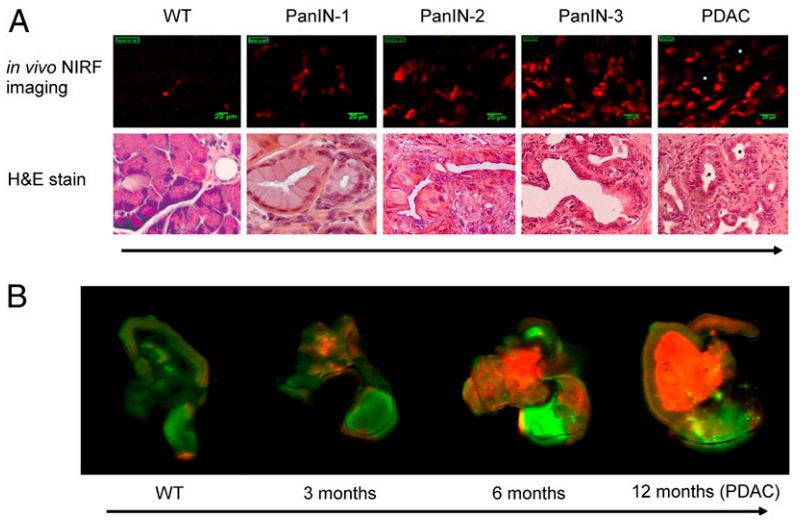

Fig. 3. Early detection of preinvasive mPanIN lesions and PDAC in vivo by flexible confocal lasermicroscopy. (*A*, *Upper*) In vivo imaging of all grades of mPanIN lesions and PDAC in *Ptf1a*$^{Cre/+}$;*LSL-Kras*$^{G12D/+}$ mice and normal pancreas in littermate controls on a cellular level using CFL and a cathepsin-activatable NIRF probe. The cathepsin-sensitive NIRF-probe signal increases with progression of mPanINs to PDAC and is almost absent in normal pancreatic tissue. Additionally, the NIRF-probe signal provides valuable information about the morphology of the lesion on a cellular level. White asterisks in the PDAC image indicate two ductal structures characteristic of PDAC in CFL. (*Lower*) The corresponding matched H&E stained histological sections are shown. Black asterisks mark the ductal structures detected by CFL in the PDAC specimen. (*B*) Ex vivo whole organ scans of the pancreas with stomach and duodenum of control and 3-, 6-, and 12-mo-old *Ptf1a*$^{Cre/+}$;*LSL-Kras*$^{G12D/+}$ animals bearing mPanIN lesions (3- and 6-mo-old mice) or PDAC (12-mo-old mouse) on a planar Odyssey near-infrared scanner. NIRF-probe signal imaged at 680 nm is shown in red. Bright field images scanned at 800 nm appear in green.

of the genotype and age of the animals and the CFL-based diagnosis. Blind analysis of the CFL recordings of the 24 individual mice by the two independent investigators correctly identified all ductal pancreatic adenocarcinomas ($n = 2$) and all cases showing normal pancreatic tissue ($n = 6$). An overall agreement of 95.8% was achieved for both investigators when comparing the diagnosis of the highest grade lesion seen on CFL recordings with grading based on histology. Interobserver agreement between the two investigators was 91.7%. Furthermore, CFL grading of the imaged pancreata correctly identified all cases that harbored mPanIN-3 lesions, demonstrating the value of the technique. For each investigator grading of mPanIN lesions on the basis of CFL recordings differed only in one case from histological findings, respectively. In each case, in vivo imaging overestimated a mPanIN-2 lesion as being mPanIN-3. However, in all cases it was possible to classify pancreata as either bearing low-grade mPanIN lesions (mPanIN-1A and -1B) versus high-grade mPanIN lesions (mPanIN-2 and -3) (Table1).

Discussion

In addition to studying tumor biology, genetically engineered mouse models are now increasingly used to conduct translational investigations. Accordingly, it was recently demonstrated that the Kras^{G12D}-dependent mouse model of PDAC accurately mimics the therapeutic response of human PDAC and thus offers the opportunity to develop novel treatments (20). Beyond testing therapeutic strategies, we now show that this model is applicable to defining novel diagnostics, which are urgently needed to detect curable lesions in the clinic. We demonstrate that CFL in combination with cathepsin-activatable NIRF probes detects premalignant pancreatic neoplasia and early-stage PDAC with high accuracy in an endogenous Kras^{G12D}-dependent mouse model of PDAC. Using a cathepsin-activatable NIRF probe and the nonspecific vascular contrast agent fluorescein, we characterized the "histopathology" of low-grade and high-grade mPanINs and early-stage PDAC in vivo, combining the advantages of the standard section (i.e. promptness in diagnosis) and immunochemistry (i.e. high sensitivity) with real-time CFL in a single-examination.

Expression of oncogenic Kras from its endogenous promoter in the pancreas of *Ptf1a*$^{Cre/+}$;*LSL-Kras*$^{G12D/+}$ mice induces the development of neoplastic changes (mPanINs and PDAC), which recapitulate the human disease in many aspects. These mice develop low-grade mPanIN lesions that progress to high-grade mPanINs and metastatic PDAC over a period of several months (14). Furthermore, desmoplastic changes similar to those seen in the human disease are regularly observed. Gene expression profiling and immunohistochemistry of mPanIN lesions and PDAC from these mice identified cathepsins as suitable targets for in vivo imaging. Cathepsins, which are known to be key factors in tumor progression and invasion (21), are also believed to play a critical role in tumor initiation (22). Consistent with the murine expression data, we detected high cathepsin expression in human preinvasive PanINs and invasive PDAC, which is in agreement with a study comprising 70 human PDAC cases. Here, 96% of primary pancreatic tumors stain positive for cathepsin B and 90% for cathepsin L (23). Therefore, our unique diagnostic strategy for the detection of high grade mPanINs can be translated directly into the clinic. Because cathepsin B and L have been shown to be independent prognostic factors of poor patient outcome in pancreatic cancer (23, 24), in vivo imaging of cathepsin activity may also provide additional information about the prognosis of the respective patient.

Using activatable NIRF probes for molecular in vivo imaging has several advantages: (*i*) in its native state the quenched probe is optically silent with no background fluorescence, minimizing false positive results; (*ii*) cleavage of multiple probes by each protease and accumulation of probes in tumors amplify the signal and increase sensitivity; (*iii*) protease recognition sites allow specific activation of probes; and (*iv*) probes can be designed to be activated by different proteases, permitting specific detection of tumors with different protease expression profiles (25). The advantages of the cathepsin-activatable NIRF probe were also observed in our study, when the molecular probe was compared with the nonspecific vascular contrast agent fluorescein, which has already been used

Downloaded at Palestinian Territory, occupied on November 26, 2021
www.manaraa.com

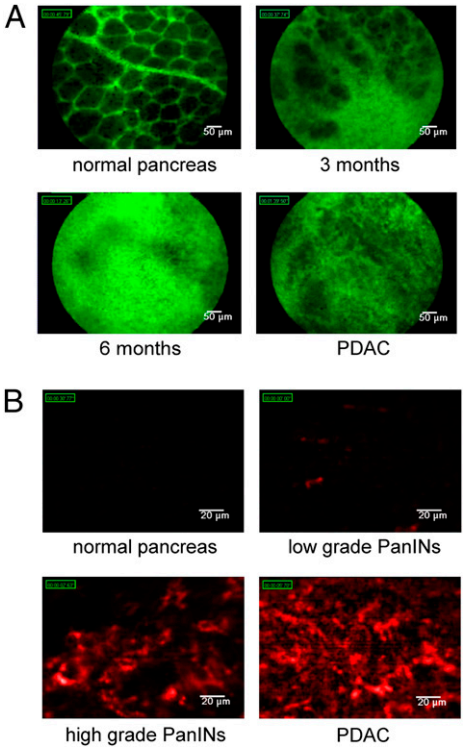

Fig. 4. Real-time dual wavelength in vivo imaging of cathepsin-activatable NIRF probes and the nonspecific vascular contrast agent fluorescein to detect mPanIN lesions and PDAC. (*A*) Flexible confocal lasermicroscopic in vivo imaging of *Ptf1a*$^{Cre/+}$;*LSL-Kras*$^{G12D/+}$ and wild-type control mice after laparatomy using the nonspecific vascular contrast agent fluorescein (green color). (Scale bar, 50 μm.) Morphology and extent of fibrosis is shown in normal pancreas, pancreas with low- (3 mo), and with high-grade mPanIN lesions (6 mo) and PDAC. (*B*) CFL imaging of cathepsin activity of *Ptf1a*$^{Cre/+}$;*LSL-Kras*$^{G12D/+}$ mice and wild-type littermate controls. (Scale bar, 20 μm.) Pictures shown depict normal pancreas, low- and high-grade mPanIN lesions, and PDAC.

for the detection of neoplastic precursor lesions and cancer in the gastrointestinal tract in humans (26–28). Morphological changes such as fibrosis, which are associated with pancreatic neoplasia, precluded the distinct detection and evaluation of mPanIN lesions and early-stage PDAC by CFL using fluorescein.

Given the poor survival rates of PDAC patients even after resection, detecting preinvasive pancreatic neoplasia and early-stage PDAC could tremendously improve survival. This is underscored by recent data showing that PanIN progression, from the initiating mutation to the emergence of the parental founder cell of the invasive carcinoma within the high-grade PanIN lesion, takes at least one decade and that another 5 to 6 y pass before cancer cells acquire metastatic capacity (13). These observations argue for a broad diagnostic window to detect curable neoplastic lesions in the pancreas and demonstrate the need for diagnostic approaches such as ours. Especially in the context of surveillance programs for familial pancreatic cancer this window can be exploited and false positive findings minimized, using our unique diagnostic imaging approach (29).

Table 1. Assessment of neoplastic changes within the pancreas by CFL in a double blind study

Histological grading	Sensitivity of CFL, %	Specificity of CFL, %
Normal pancreas	100	100
PanIN-1	100	100
PanIN-2	75.0	100
PanIN-3	100	95.4
PDAC	100	100

Accuracy of detecting and grading neoplastic changes within the pancreas on the basis of in vivo CFL studies with the cathepsin-activatable NIRF probe was determined in a total of 24 mice in a double blind study (*Materials and Methods* for study design). Overall agreement of 95.8% was achieved by each of two independent blinded investigators when comparing CFL-based diagnosis of highest grade lesion observed (i.e., no lesion, mPanIN-1, -2, or -3, and PDAC) with diagnosis on the basis of serial histological sections. Interobserver agreement over all cases was 91.7%. Sensitivity and specificity of CFL-based histopathological diagnoses compared with gold standard H&E diagnoses are shown for each grade of PanIN, PDAC, and normal pancreatic tissue.

Preinvasive PanIN lesions are the most common precursors to invasive PDAC, rendering them promising targets for diagnosis and intervention, especially in the high-risk population (30). Using CFL in combination with an established cathepsin-activatable NIRF probe allowed us to distinguish between different grades of mPanIN lesions by signal intensity, cellular morphology, and pattern of activation. Thus, it was possible to differentiate on the cellular level between low-grade mPanINs, which on the basis of current knowledge do not require treatment and high-grade mPanIN lesions and early-stage PDAC, requiring therapeutic intervention (11, 31). This differentiation is essential in the management of high-risk individuals who show suspicious changes within the pancreas in endoscopic ultrasound (EUS) or other imaging studies. Because many high-risk individuals show pancreatitis-like changes within the pancreas, differentiation between these irregularities and high-grade PanINs and PDAC is important (12, 32). In the future, these lesions can be evaluated by in vivo CFL using targeted probes to improve diagnostic accuracy. This improvement may significantly decrease overtreatment of persons at risk for PDAC.

The approach we have demonstrated in mice has the capacity to be translated into clinical medicine. First, the confocal lasermicroscopic imaging system is US Food and Drug Administration (FDA) approved and Conformité Européenne (CE) marked. Second, the cathepsin-activatable NIRF probe shows no toxic side effects when applied i.v. and is currently being reviewed for FDA approval (18). Given the compatibility of the flexible confocal lasermicroscope with any conventional endoscope, our approach can be incorporated into a regular endoscopic examination. However, the translation from our model to clinical practice faces the problem of accessibility of the pancreas in humans, which needs to be resolved. However, this problem can be overcome by advancing the confocal lasermicroscope through a 19-G fine needle used for EUS guided puncture of the pancreas. This procedure allows the examiner to obtain an "in vivo histopathology" of nondisrupted tissue and subsequently obtain targeted biopsies. The feasibility of this EUS guided approach was recently shown by our group in a porcine large-animal model using fluorescein as a vascular contrast agent (33). Additionally the small size of the confocal lasermicroscope allows the intubation of the main pancreatic duct during endoscopic retrograde pancreaticoscopy as has already been shown in humans by our group (34). Furthermore, the diagnostic approach we describe here may also help to refine laparoscopic staging and surgical resection of PanINs and PDAC by improving intraoperative localization and evaluation of suspicious lesions and assessment of resection margins on a cellular level in real time during surgery (35). Finally, CFL in combination with the established activatable NIRF probe should be used to image other gastrointestinal neoplasias, many of which are more easily accessible than those of the pancreas (36–38).

Taken together, our data demonstrate the power of activatable cathepsin-sensing NIRF probes for fluorescence-guided molecular endoscopy. Utilization of this technique enables the detection and evaluation of early precursors of PDAC in vivo, holding great promise to improve early detection of PDAC and provide a basis

Downloaded at Palestinian Territory, occupied on November 26, 2021
www.manaraa.com

on which individuals at risk for PDAC can be monitored and treated successfully.

Materials and Methods

Mouse Strains and Tumor Models. The *LSL-Kras^{G12D}* (39) and *Ptf1a$^{Cre/+}$* (40) mice were previously described. The strains were interbred to obtain *Ptf1a$^{Cre/+}$;LSL-Kras^{G12D}* mice. Acute pancreatitis was induced as described (16, 41). All animal studies were conducted in compliance with European guidelines for the care and use of laboratory animals and were approved by the local authorities.

Gene Expression Profiling. mRNA expression profiles were generated using GeneChip Mouse Genome 430 2.0 arrays (Affymetrix) as recently described (16, 42) (*SI Materials and Methods*).

Histology and Immunohistochemistry. Formalin-fixed paraffin-embedded tissue sections were H&E stained or stained with anti-cathepsin B (1:50), anti-cathepsin H (1:40), anti-cathepsin L (1:40), or anti-cathepsin S (1:40) (R&D Systems) as described (43, 44) (*SI Materials and Methods*).

Confocal Laserscanning Microscopy. Confocal microscopy was performed on cryosections (*SI Materials and Methods*), stained with an anti–E-cadherin antibody (diluted 1:80, AF-748; R&D Systems), followed by an Alexa Fluor 555-labeled secondary antibody (Invitrogen). Stained sections were analyzed with a confocal laserscanning microscope (Leica; SP5).

Application of NIRF Probes and Fluorescein. Mice were injected i.v. with either 150 μL (2 nm) of a cathepsin B/H/L/S sensitive probe (ProSense 680) (VisEn Medical) as described (16) or 100 μL 0.05% fluorescein.

In Vivo CFL. CFL was performed as described (16) using the Cellvizio488 and 660 Laser Scanning units (Mauna Kea Technologies) for fluorescein and cathepsin NIRF-probe imaging, respectively (*SI Materials and Methods*).

Ex Vivo Fluorescence Imaging. Ex vivo imaging was performed as described (16, 44) on an Odyssey near-infrared reader (Li-Cor) at 680 nm for probe-specific fluorescence and at 800 nm for bright field imaging (*SI Materials and Methods*).

Animal Study Design. The potential of in vivo CFL imaging to detect and grade neoplastic changes within the pancreas was evaluated in a blind study. Mice of varying age, bearing neoplastic changes spanning the whole spectrum from mPanIN-1A to PDAC ($n = 18$) or normal littermate controls ($n = 6$), were imaged in vivo using the cathepsin-activatable NIRF probe. Imaging-based diagnoses were compared with histological diagnoses (*SI Materials and Methods*).

ACKNOWLEDGMENTS. We thank Dr. T. Jacks and Dr. D. Tuveson for *LSL-Kras^{G12D}* mice; Dr. H. Nakhai for *Ptf1a$^{Cre/+}$* mice; Dr. Florian Nagl for assistance with imaging studies; and U. Götz, M. Werb, and M. Göbel for excellent technical assistance. This study was supported by Deutsche Krebshilfe (Project 108985, to D.S.), Deutsche Forschungsgemeinschaft (Sonderforschungsbereich 824, Teilprojekt C9, to D.S. and G.S.), and Bundesministerium für Bildung und Forschung, MoBiMed Programm (01 EZ 0802, to D.S. and A.E.S.).

1. Schneider G, Siveke JT, Eckel F, Schmid RM (2005) Pancreatic cancer: Basic and clinical aspects. *Gastroenterology* 128:1606–1625.
2. Furukawa H, et al. (1996) Clinicopathologic features of small pancreatic adenocarcinoma. A collective study. *Cancer* 78:986–990.
3. Agarwal B, Correa AM, Ho L (2008) Survival in pancreatic carcinoma based on tumor size. *Pancreas* 36:e15–e20.
4. Shimada K, Sakamoto Y, Sano T, Kosuge T, Hiraoka N (2006) Reappraisal of the clinical significance of tumor size in patients with pancreatic ductal carcinoma. *Pancreas* 33: 233–239.
5. Shimizu Y, Yasui K, Matsueda K, Yanagisawa A, Yamao K (2005) Small carcinoma of the pancreas is curable: New computed tomography finding, pathological study and postoperative results from a single institute. *J Gastroenterol Hepatol* 20:1591–1594.
6. Rulyak SJ, Lowenfels AB, Maisonneuve P, Brentnall TA (2003) Risk factors for the development of pancreatic cancer in familial pancreatic cancer kindreds. *Gastroenterology* 124:1292–1299.
7. Raimondi S, Maisonneuve P, Lowenfels AB (2009) Epidemiology of pancreatic cancer: An overview. *Nat Rev Gastroenterol Hepatol* 6:699–708.
8. Lichtenstein P, et al. (2000) Environmental and heritable factors in the causation of cancer—analyses of cohorts of twins from Sweden, Denmark, and Finland. *N Engl J Med* 343:78–85.
9. Chu D, Kohlmann W, Adler DG (2010) Identification and screening of individuals at increased risk for pancreatic cancer with emphasis on known environmental and genetic factors and hereditary syndromes. *JOP* 11:203–212.
10. Brand RE, et al.; Participants of the Fourth International Symposium of Inherited Diseases of the Pancreas (2007) Advances in counselling and surveillance of patients at risk for pancreatic cancer. *Gut* 56:1460–1469.
11. Hruban RH, Maitra A, Kern SE, Goggins M (2007) Precursors to pancreatic cancer. *Gastroenterol Clin North Am* 36:831–849, vi.
12. Canto MI, et al. (2006) Screening for early pancreatic neoplasia in high-risk individuals: A prospective controlled study. *Clin Gastroenterol Hepatol* 4:766–781, quiz 665.
13. Yachida S, et al. (2010) Distant metastasis occurs late during the genetic evolution of pancreatic cancer. *Nature* 467:1114–1117.
14. Hingorani SR, et al. (2003) Preinvasive and invasive ductal pancreatic cancer and its early detection in the mouse. *Cancer Cell* 4:437–450.
15. Frese KK, Tuveson DA (2007) Maximizing mouse cancer models. *Nat Rev Cancer* 7: 645–658.
16. von Burstin J, et al. (2008) Highly sensitive detection of early-stage pancreatic cancer by multimodal near-infrared molecular imaging in living mice. *Int J Cancer* 123:2138–2147.
17. Weissleder R, Tung CH, Mahmood U, Bogdanov A, Jr. (1999) In vivo imaging of tumors with protease-activated near-infrared fluorescent probes. *Nat Biotechnol* 17:375–378.
18. Ignat M, et al. (2009) Feasibility and reliability of pancreatic cancer staging using fiberoptic confocal fluorescence microscopy in rats. *Gastroenterology* 137:1584–1592, e1.
19. Becker V, et al. (2007) High-resolution miniprobe-based confocal microscopy in combination with video mosaicing (with video). *Gastrointest Endosc* 66:1001–1007.
20. Olive KP, et al. (2009) Inhibition of Hedgehog signaling enhances delivery of chemotherapy in a mouse model of pancreatic cancer. *Science* 324:1457–1461.
21. Gocheva V, Joyce JA (2007) Cysteine cathepsins and the cutting edge of cancer invasion. *Cell Cycle* 6:60–64.
22. Gocheva V, et al. (2006) Distinct roles for cysteine cathepsin genes in multistage tumorigenesis. *Genes Dev* 20:543–556.
23. Niedergethmann M, et al. (2004) Prognostic impact of cysteine proteases cathepsin B and cathepsin L in pancreatic adenocarcinoma. *Pancreas* 29:204–211.
24. Joyce JA, et al. (2004) Cathepsin cysteine proteases are effectors of invasive growth and angiogenesis during multistage tumorigenesis. *Cancer Cell* 5:443–453.
25. Weissleder R, Ntziachristos V (2003) Shedding light onto live molecular targets. *Nat Med* 9:123–128.
26. Kiesslich R, et al. (2004) Confocal laser endoscopy for diagnosing intraepithelial neoplasias and colorectal cancer in vivo. *Gastroenterology* 127:706–713.
27. Kiesslich R, et al. (2006) In vivo histology of Barrett's esophagus and associated neoplasia by confocal laser endomicroscopy. *Clin Gastroenterol Hepatol* 4:979–987.
28. Meining A, et al. (2007) In vivo histopathology for detection of gastrointestinal neoplasia with a portable, confocal miniprobe: An examiner blinded analysis. *Clin Gastroenterol Hepatol* 5:1261–1267.
29. Greenhalf W, Grocock C, Harcus M, Neoptolemos J (2009) Screening of high-risk families for pancreatic cancer. *Pancreatology* 9:215–222.
30. Hruban RH, Maitra A, Goggins M (2008) Update on pancreatic intraepithelial neoplasia. *Int J Clin Exp Pathol* 1:306–316.
31. Klöppel G, Lüttges J (2004) The pathology of ductal-type pancreatic carcinomas and pancreatic intraepithelial neoplasia: Insights for clinicians. *Curr Gastroenterol Rep* 6:111–118.
32. Langer P, et al. (2009) Five years of prospective screening of high-risk individuals from families with familial pancreatic cancer. *Gut* 58:1410–1418.
33. Becker V, et al. (2010) Needle-based confocal endomicroscopy for in vivo histology of intra-abdominal organs: First results in a porcine model (with videos). *Gastrointest Endosc* 71:1260–1266.
34. Meining A, Phillip V, Gaa J, Prinz C, Schmid RM (2009) Pancreaticoscopy with miniprobe-based confocal laser-scanning microscopy of an intraductal papillary mucinous neoplasm (with video). *Gastrointest Endosc* 69:1178–1180.
35. Sheth RA, et al. (2009) Improved detection of ovarian cancer metastases by intraoperative quantitative fluorescence protease imaging in a pre-clinical model. *Gynecol Oncol* 112: 616–622.
36. Alencar H, et al. (2007) Colonic adenocarcinomas: Near-infrared microcatheter imaging of smart probes for early detection—study in mice. *Radiology* 244:232–238.
37. Funovics MA, Alencar H, Montet X, Weissleder R, Mahmood U (2006) Simultaneous fluorescence imaging of protease expression and vascularity during murine colonoscopy for colonic lesion characterization. *Gastrointest Endosc* 64:589–597.
38. Wang TD (2010) Targeted imaging of flat and depressed colonic neoplasms. *Gastrointest Endosc Clin N Am* 20:579–583.
39. Jackson EL, et al. (2001) Analysis of lung tumor initiation and progression using conditional expression of oncogenic K-ras. *Genes Dev* 15:3243–3248.
40. Nakhai H, et al. (2007) Ptf1a is essential for the differentiation of GABAergic and glycinergic amacrine cells and horizontal cells in the mouse retina. *Development* 134: 1151–1160.
41. Algül H, et al. (2007) Pancreas-specific RelA/p65 truncation increases susceptibility of acini to inflammation-associated cell death following cerulein pancreatitis. *J Clin Invest* 117:1490–1501.
42. Reichert M, Saur D, Hamacher R, Schmid RM, Schneider G (2007) Phosphoinositide-3-kinase signaling controls S-phase kinase-associated protein 2 transcription via E2F1 in pancreatic ductal adenocarcinoma cells. *Cancer Res* 67:4149–4156.
43. Seidler B, et al. (2008) A Cre-loxP-based mouse model for conditional somatic gene expression and knockdown in vivo by using avian retroviral vectors. *Proc Natl Acad Sci USA* 105:10137–10142.
44. von Burstin J, et al. (2009) E-cadherin regulates metastasis of pancreatic cancer in vivo and is suppressed by a SNAIL/HDAC1/HDAC2 repressor complex. *Gastroenterology* 137:361–371, 371.e1–e5.

Downloaded at Palestinian Territory, occupied on November 26, 2021
www.manaraa.com